Quaternary Science Reviews 155 (2017) 67–78

Contents lists available at ScienceDirect

Quaternary Science Reviews

journal homepage: www.elsevier.com/locate/quascirev

Episodic Neoglacial snowline descent and glacier expansion on Svalbard reconstructed from the ^{14}C ages of ice-entombed plants

Gifford H. Miller [a, b, c, *], Jon Y. Landvik [d], Scott J. Lehman [a], John R. Southon [e]

[a] Institute of Arctic and Alpine Research, University of Colorado Boulder, 80309-0450, USA
[b] Dept. Geological Sciences, University of Colorado Boulder, 80309-0399, USA
[c] Dept. Environment & Agriculture, Curtin University, Perth, WA 6102, Australia
[d] Dept. Environmental Sciences, Norwegian University of Life Sciences, Box 5003, NO-1432 Aas, Norway
[e] Earth System Science Dept., University of California Irvine, 92697, USA

ARTICLE INFO

Article history:
Received 3 January 2016
Received in revised form
31 October 2016
Accepted 31 October 2016
Available online 23 November 2016

Keywords:
Svalbard
Neoglaciation
Radiocarbon
Holocene
Recent warming
Glacier
Climate
Little Ice Age
Medieval

ABSTRACT

The response of the Northern Hemisphere cryosphere to the monotonic decline in summer insolation and variable radiative forcing during the Holocene has been one of irregular expansion culminating in the Little Ice Age, when most glaciers attained their maximum late Holocene dimensions. Although periods of intervening still-stand or ice-retreat can be reconstructed by direct dating of ice-recessional features, defining times of Neoglacial ice growth has been limited to indirect proxies preserved in distal archives. Here we report 45 precise radiocarbon dates on *in situ* plants emerging from beneath receding glaciers on Svalbard that directly date the onset of snowline descent and glacier expansion, entombing the plants. Persistent snowline lowering occurred between 4.0 and 3.4 ka, but with little additional persistent lowering until early in the first millennium AD. Populations of individual ^{14}C calendar age results and their aggregate calendar age probabilities define discrete episodes of vegetation kill and snowline lowering 240–340 AD, 410–540 AD and 670–750 AD, each with a lower snowline than the preceding episode, followed by additional snowline lowering between 1000 and 1220 AD, and between 1300 and 1450 AD. Snowline changes after 1450 AD, including the maximum ice extent of the Little Ice Age are not resolved by our collections, although snowlines remained lower than their 1450 AD level until the onset of modern warming. A time-distance diagram derived from a 250-m-long transect of dated ice-killed plants documents ice-margin advances ~750, ~1100 and after ~1500 AD, concordant with distributed vegetation kill ages seen in the aggregate data set, supporting our central thesis that vegetation kill ages provide direct evidence of snowline lowering and cryospheric expansion. The mid- to late-Holocene history of snowline lowering on Svalbard is similar to ELA reconstructions of Norwegian and Svalbard cirque glaciers, and consistent with a cryospheric response to the secular decline of regional summertime insolation and stepped changes in nearby surface ocean environments. The widespread exposure of entombed plants dating from the first millennium AD suggests that Svalbard's average summer temperatures of the past century now exceed those of any century since at least 700 AD, including medieval times.

1. Introduction

The Svalbard archipelago (Fig. 1) is one of the most northerly island groups in the Northern Hemisphere (NH), with a land surface that is presently ~60% glaciated (Hagen et al., 1993). During the Last Glacial Maximum (~21 ka) ice extended onto the adjacent continental shelves and the subsequent deglaciation history has been relatively well documented based on a combination of glacial and marine geologic studies (Landvik et al., 1998). However, the record of more recent Late Holocene climate history and associated ice cap and glacier variation remains fragmentary, in large part because most Svalbard glaciers reached their maximum Neoglacial

* Corresponding author. Institute of Arctic and Alpine Research, University of Colorado Boulder, 80309-0450, USA.
E-mail addresses: gmiller@colorado.edu (G.H. Miller), jon.landvik@nmbu.no (J.Y. Landvik), scott.lehman@colorado.edu (S.J. Lehman), jsouthon@uci.edu (J.R. Southon).

http://dx.doi.org/10.1016/j.quascirev.2016.10.023
0277-3791/

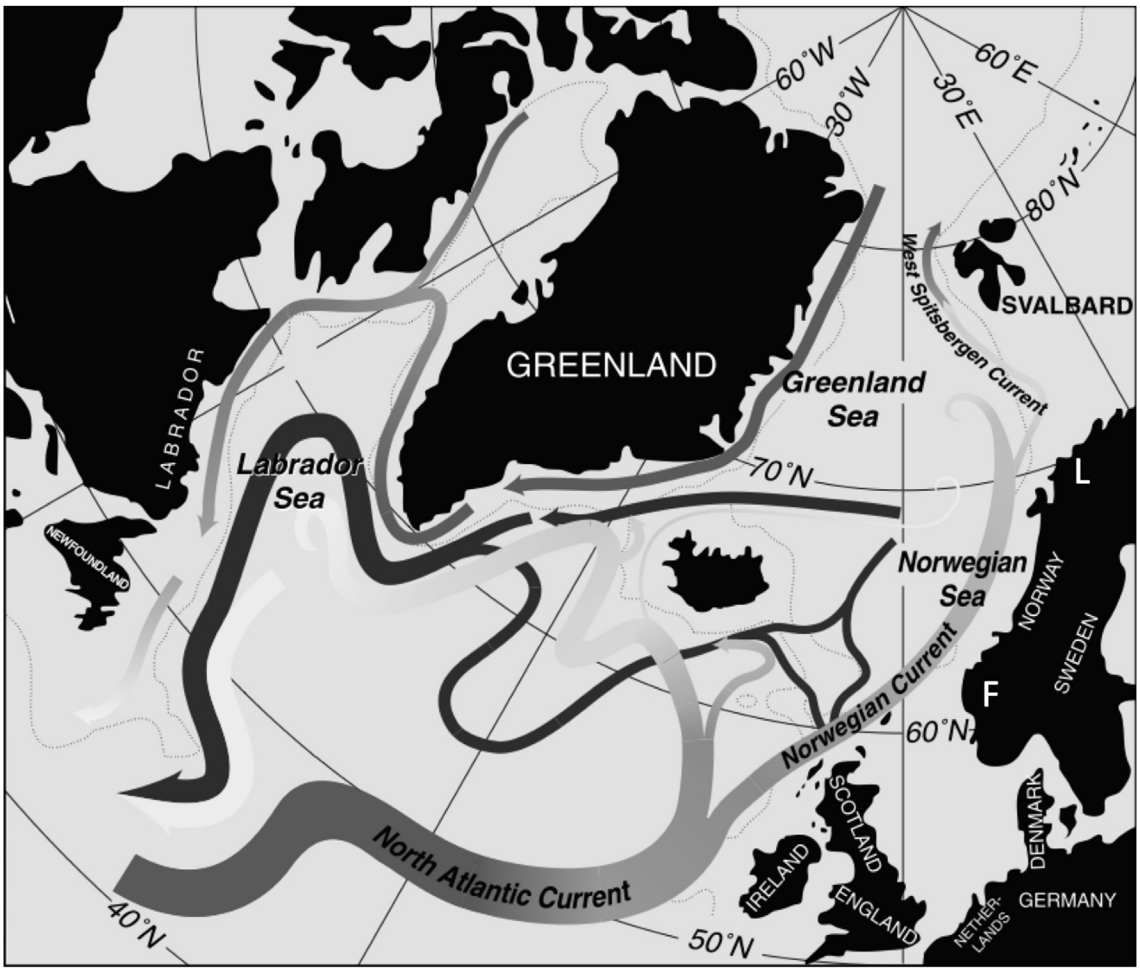

Fig. 1. Northern North Atlantic region, showing the location of Svalbard and major North Atlantic surface currents; warm surface currents (light tones), cold surface currents (darker tones), deep currents (darkest tones). L: Lenangsbreene; F: Folgefonna. Modified from (McCartney et al., 1996).

extent during the Little Ice Age (LIA; Svendsen and Mangerud, 1997) removing evidence of earlier advances. Rare remnant lateral moraines indicate multiple Neoglacial advances, but dating moraine formation has proven to be challenging. Werner (1993) used lichenometry to provide approximate ages on nested Neoglacial moraines fronting Svalbard glaciers, documenting at least four advances, with moraine stabilization ~1.5 ka, ~1.0 ka, ~0.6 ka and around the end of the 19th Century. Cosmogenic radionuclides in boulders from a remnant lateral moraine on Spitsbergen suggest moraine stabilization there at about 1.6 ka (Reusche et al., 2014), although ages were highly variable indicating that they may have been influenced by nuclide inheritance and post-depositional rotation of moraine boulders. Changes in Svalbard glacier activity also has been inferred from diagnostic proxies preserved in glacier-dominated lake sediments (Svendsen and Mangerud, 1997; Snyder et al., 2000b; Røthe et al., 2015), indicating Neoglaciation began ~5 ka, with local glaciers reaching maximum dimensions in the LIA.

Repeat aerial and satellite surveys of Svalbard glaciers document significant lateral glacier retreat since their LIA maximum (Hagen et al., 2003), with an estimated further reduction of glacierized area of ~7% in the last ~30 years (Nuth et al., 2013). Retreat of Svalbard glaciers coincides with an interval of rising summer temperatures, which have increased locally by more than 0.5 °C per decade since 1980 (Fig. 2). In parts of western Svalbard, glacier retreat appears to have been aggravated by upland ice cap thinning attributable to a recent decrease in winter-time precipitation (James et al., 2012). The temperature of the Svalbard Archipelago is maintained well above the zonal average by the presence of the warm, poleward flowing West Spitsbergen Current (WSC), a northerly extension of the North Atlantic Current (Fig. 1) related in part to the Atlantic Meridional Overturning Circulation (AMOC). The associated heat transport results in mean annual surface air temperatures (MAT) over Svalbard that are ~10 °C higher than over NE Greenland, <500 km distant at the same latitude. Earlier studies have noted a correlation between the instrumental MAT record over the Arctic (Chylek et al., 2009) and Svalbard (Humlum et al., 2011) and the Atlantic Multi-decadal Oscillation (AMO) index, a basin-wide average of North Atlantic sea surface temperature (SST), thought to represent a response to internal or forced variability of the AMOC and changes in the bulk planetary radiative forcing (Hurrell and Deser, 2010). We note a zero-lag correlation of the record of yearly summertime Svalbard temperature (Fig. 2) and the AMO since 1899 of 0.42, but a substantially larger correlation ($R = 0.60$) with the record of annual average extra-tropical Northern Hemisphere temperature (of which the local record is only a very small part). This, together with the fact that indices of AMOC strength have declined in recent decades (Rahmstorf et al., 2015) while Svalbard temperatures have continued to rise, suggest that local temperatures are substantially influenced by altered radiative forcing in addition to variable ocean heat transport. On longer timescales, the regular decline in local summer insolation receipts also influenced Arctic temperature and ice extent through

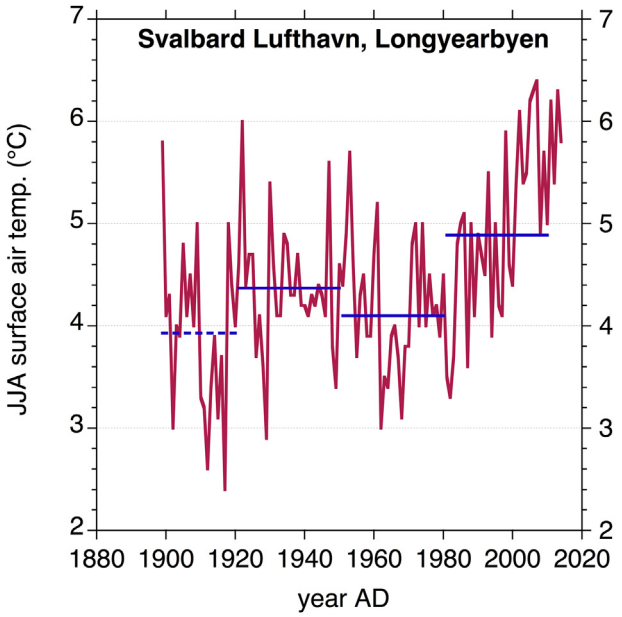

Fig. 2. Mean summer air temperature (for June, July and August) measured at Longyearbyen Airport (Lufthavn) since 1899 AD (Nordli et al., 2014). Horizontal (blue) bars represent 30-year averages (shorter for the interval ending in 1920). The relatively warm tri-decade 1981–2010 corresponds to an interval of significant ice loss over Svalbard (~7% by area, Nuth et al., 2013); summer warming and ice loss appear to be accelerating. (For interpretation of the references to colour in this figure legend, the reader is referred to the web version of this article.)

the Holocene (e.g., Kaufman et al., 2004).

In this study we capitalize on the consequences of recent summer warming which has led to the emergence of intact tundra plants from beneath retreating ice margins. The ^{14}C ages of these long-dead plants define when the plant was killed by the lowering of regional snowline, either immediately by *in situ* transformation of snow to glacier ice at the ice margin or soon after by related advance of cold-based ice (Miller et al., 2013a). In either case, kill dates define an expansion of the cryosphere resulting from persistent summer cooling. Here we report 45 precise non-modern (52 total) radiocarbon dates on formerly ice-entombed plants from central West Spitsbergen, Svalbard which we use to reconstruct relative changes in elevation of the regional snowline or equilibrium line altitude since the onset of Neoglaciation, which began locally ~4 ka BP as indicated by the age of the oldest samples in our collections.

2. Ice-entombed plants emerging beneath receding ice margins date past episodes of snowline depression

In 1963 the Canadian geologist George Falconer discovered *Polytrichum* moss *in situ* appearing beneath the margin of a thin ice cap on the central plateau of Baffin Island, Arctic Canada (Falconer, 1966). A radiocarbon date on the moss suggested the plants were entombed by ice during the LIA, and had been preserved intact for centuries. His observation suggested that many of the other thin, cold-based plateau ice caps in the region might also preserve ancient ecosystems. Two decades later a rich community of Arctic plants was found emerging beneath a glacier snout in the Canadian High Arctic (Bergsma et al., 1984), with radiocarbon dates on the plants similar to that reported by Falconer, 1966, suggesting ice advanced over the plants during the LIA, entombing them until they were exposed shortly before they were collected. Fifteen years later, *in situ* dead moss was reported at the margins and in kill zones beyond the margins of glaciers on Franz Josef Land (Lubinski et al., 1999). Radiocarbon dates on ten of those samples indicated glaciers expanded shortly after 1000 AD, with increased expansion after 1450 AD.

More recently, tundra plants were found preserved beneath Longyearbreen, a 5-km-long glacier in central Spitsbergen (Fig. 3; Humlum et al., 2011). Subglacial access was provided by an abandoned moulin connected to a complex of disused subglacial meltwater tunnels, 2 km from the glacier terminus. Vascular plants and moss were found *in situ* in soils flooring the abandoned conduits. Eleven samples of bryophyte taxa dated from the first millennium AD, with calibrated ages indicating that Longyearbreen advanced across the site no later than 780 AD, well before the LIA, and remained in an expanded state through to the present, although the glacier is currently melting rapidly.

Building on the observations of Falconer (1966), Anderson et al. (2008) visited numerous other small plateau ice caps on central Baffin Island and found *in situ* tundra plants emerging along most ice margins. That work was geographically expanded by Miller et al. (2012, 2013b), and Margreth et al. (2014) following recognition that even large coastal ice caps preserve ancient plants. The greatly expanded geographic and elevational range provided by the extensive suite of coastal ice caps along the eastern rim of Baffin Island resulted in a wider range of kill dates, with emerging plants as old as 5 ka (Margreth et al., 2014; Miller et al., 2013b), and at four different ice caps replicate analyses of emerging moss were >40 ka, at or near the limit of radiocarbon dating (Miller et al., 2013b). Recently, dead plants also have been reported at and nearby ice margins in East Greenland (Lowell et al., 2013).

3. Field area

With the realization that *in situ* tundra plants were emerging beneath receding glaciers across several regions of the North Atlantic Arctic, including subglacial plants on Svalbard, we initiated a search for rooted plants emerging beneath receding ice margins on Svalbard. We targeted optimal sites for plant preservation based on high-resolution Digital Globe imagery provided by Polar Geospatial Center (http://www.pgc.umn.edu) and aerial photographs. Past experience leads us to target sites with vegetation-kill trimlines, which demonstrate significant lateral retreat in recent decades, and inliers of exposed ice-free land, which commonly escape erosion by basal ice and ice-marginal streams. We restricted potential collection sites to regions of the main island, Spitsbergen, that lie outside protected areas, with final target selection based on weather. Fig. 3 shows the location of sample sites; site coordinates are given in Table 1. Late-lying seasonal snow can be a complicating factor. During our 2013 field campaign we found that partially refrozen snow challenged our ability to securely identify the glacier margin in some areas.

4. Methods

We made 60 collections of dead plants along ice margins on Spitsbergen. At each site we target *in situ* moss following guidelines outlined in Miller et al. (2013a,b), making two (or more) collections, usually separated by tens of meters, to allow for multiple, independent measurements. We avoid sampling woody plants because their survival potential is much greater than for moss, and their woody stems carry an average radiocarbon age older than their kill date. For example, radiocarbon ages on three adjacent *in situ* plants emerging beneath a glacier in the Canadian High Arctic include two moss taxa for which the dates are concordant, and a date on *Salix*, the arctic willow, that is 200 years older (LaFarge et al., 2013). Hence, woody plant kill-dates might be from non-climate causes,

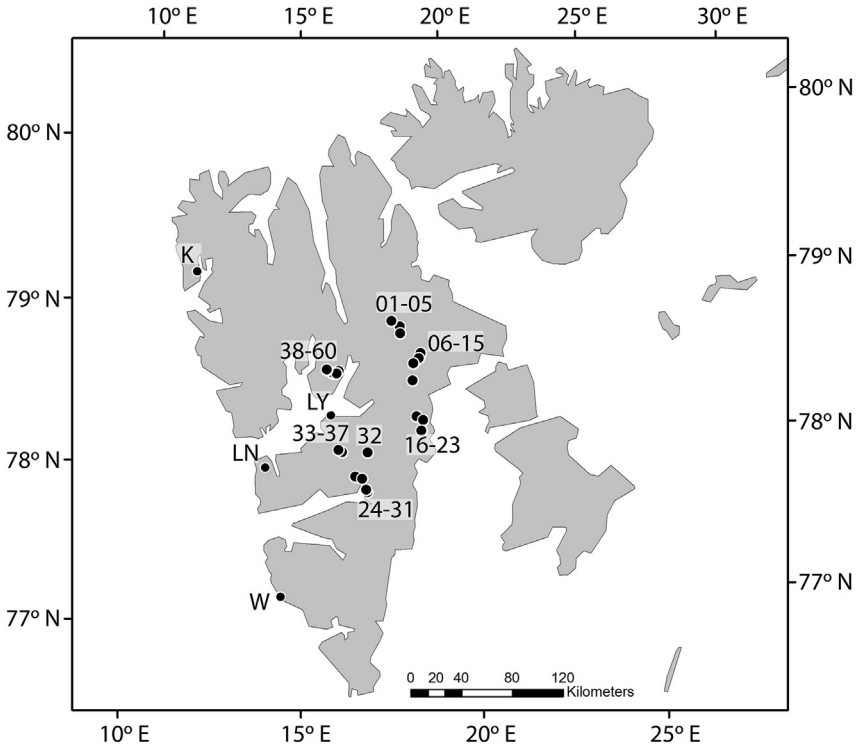

Fig. 3. Map of Svalbard with dead moss collection sites located by Field ID (Table 1). Locations of Longyearbreen and the town of Longyearbyen (LY), Linnévatnet (LN), Karlbreen (K), Werenskioldbreen (W) are indicated.

whereas mosses that die naturally are rapidly lost from the landscape in most settings. Whenever possible, we restrict our sampling to within 1 m of the current ice margin. Collections that close to the ice usually sample plants that were exposed the same year as they were collected, given current melt rates.

Ice-proximal sampling is important because even dead moss may re-grow upon emergence. Mosses regenerate sexually from spores and vegetatively by sprouting from specialized gametophyte tissues and from stem fragments and rhizoids (Hobbs et al., 1984). Desiccated moss stems that emerged beneath ice after 400 years entombment in the Canadian High Arctic were observed to regenerate spontaneously in the field and in the laboratory after grinding stems and leaves and sowing on growth media (LaFarge et al., 2013). Collecting <1 m from the ice margin limits the probability of any new growth in our samples.

Samples were kept refrigerated after collection, and then freeze-dried shortly after the field season. To prepare a sample for radiocarbon dating, each freeze-dried sample was rehydrated, gently sonicated, and where possible, a single stem of sufficient mass was selected for dating to minimize the chance of dating a mixed-age sample. The dried stem(s) selected for dating was then treated with an acid-base-acid wash, combusted, and converted to graphite at the INSTAAR radiocarbon laboratory (NSRL: http://instaar.colorado.edu/research/labs-groups/laboratory-for-ams-radiocarbon-preparation-and-research/). Packed targets were measured at the W.M. Keck Carbon Cycle Accelerator Mass Spectrometry Laboratory at the University of California Irvine. Radiocarbon dates were calibrated using OxCal 4.2 and IntCal13 (Bronk Ramsey et al., 2012); they are reported as conventional radiocarbon ages ±1σ, and as calibrated median ages with ±1σ ranges (Table 1). Ages discussed in the text and given in figures are expressed in calibrated years AD for samples younger than 2000 calendar years BP and in calibrated years or kiloyears (ka) BP for older ages.

5. Results

We found *in situ* tundra plants close to current ice-cap margins at most of our targeted sites. At some sites, plants were found in great abundance, at others only in protected settings (Fig. 4). We obtained 52 radiocarbon dates from these collections (Table 1). Samples from four sites returned excess ^{14}C concentrations ($F_m > 1$; Table 1), and hence must have been killed after the onset of atmospheric nuclear testing in the late 1940's. Adjacent collections of securely dead moss (samples 27, 28 and samples 29, 30) and replicate stems of collection 17 all had $F_m > 1$, whereas moss from sample 7 was dated twice, with $F_m > 1$ in an initial date, but a second date is 1130 AD, suggesting some regrowth may have occurred after initial emergence. All seven samples with $F_m > 1$ fall in a range indicative of kill-dates early in the atmospheric bomb-testing era. Hence, we speculate that they were killed by snowline lowering during an interval of summer cooling between 1950 and 1961 (Fig. 2), and that late-lying seasonal snow obscured the glacier margin. They are omitted from the discussions that follow.

5.1. Distribution of calibrated ages

To evaluate whether our measurements reflect an unstructured progression of dates, or if groupings are present, we plot median calibrated age and ±1σ range for all non-modern samples in rank order (youngest to oldest), along with the elevation of each collection (Fig. 5). Despite the wide geographic range of our collections and the varying size of associated ice bodies, there remains a statistically significant, positive relationship ($r = 0.62$, $p < 0.01$) between sample elevation and age, as may be expected in response to the long term decline in regional summertime insolation (and, consequently, of summer temperature and snowline). However, the distribution of ages in time also contains distinct breaks that define series or groupings of dates corresponding to moss kill intervals.

Table 1
Tabulation of 52 radiocarbon dates on dead moss recently emerged from beneath glacier ice on Svalbard and their metadata. Field IDs refer to Fig. 3. Calibrated ages from OxCal 4.2 with ± ranges representing one-sigma uncertainties. Distance from the current ice margin where known is given as "Ice Edge".

Lab ID	Field ID	Elevation (m asl)	Ice Edge (m)	Lat (°N)	Long (°W)	$\delta^{13}C$	^{14}C Age	±	Median Cal Age BP	±	Median Cal Age AD	±
NSRL-24208	NC13-S015	650	0.1	78.54200	18.49775	−32.9‰	135	20	130	130	1810	130
NSRL-24748	NC13-S004	1196	Unk	78.91578	17.90889	−26.2‰	135	20	130	120	1810	130
NSRL-24205	NC13-S004	1196	Unk	78.91578	17.90889	−29.7‰	150	20	180	140	1800	130
NSRL-24752	NC13-S014	655	1	78.54268	18.49725	−28.9‰	195	20	170	135	1780	145
NSRL-24199	NC13-S045	646	250	78.60662	15.99926	−26.0‰	290	20	395	70	1580	60
NSRL-25290	NC13-S018	375	0	78.29433	18.75873	−25.5‰	415	15	500	10	1460	10
NSRL-24197	NC13-S041	544	3	78.61704	16.19211	−32.0‰	450	20	510	20	1440	5
NSRL-24196	NC13-S040	543	1	78.61750	16.19195	−28.7‰	460	20	515	20	1440	5
NSRL-25291	NC13-S022	382	0.2	78.22851	18.68557	−24.1‰	480	20	520	10	1430	10
NSRL-25296	NC13-S042	547	0.4	78.61747	16.19246	−29.2‰	545	15	545	10	1395	15
NSRL-25294	NC13-S038	546	3	78.61701	16.19219	−23.9‰	590	20	605	40	1350	40
NSRL-24201	NC13-S052	688	120	78.60118	16.12338	−27.0‰	660	20	600	55	1335	45
NSRL-25295	NC13-S039	542	3	78.61749	16.19201	−23.0‰	665	15	650	50	1330	55
NSRL-24754	NC13-S023	384	0.2	78.22919	18.68466	−24.0‰	670	20	650	55	1325	50
NSRL-24210	NC13-S019	373	0	78.29425	18.76063	−29.4‰	825	20	730	50	1220	20
NSRL-24211	NC13-S021	379	0.15	78.22818	18.69335	−29.4‰	850	20	755	50	1195	25
NSRL-25289	NC13-S013	437	0.2	78.64959	18.53723	−21.4‰	860	15	760	20	1190	20
NSRL-24749	NC13-S007	568	0	78.70938	18.78562	−24.8‰	890	25	800	60	1130	75
NSRL-24740	NC13-S046	639	115	78.60549	16.00107	−22.6‰	910	20	860	40	1105	55
NSRL-24741	NC13-S047	633	65	78.60509	16.00205	−26.0‰	955	20	850	50	1090	60
NSRL-24217	NC13-S037	703	0.1	78.12686	16.14180	−25.7‰	1020	20	940	25	1010	15
NSRL-24204	NC13-S002	729	0.5	78.88099	18.17039	−28.1‰	1040	20	950	25	1000	10
NSRL-24198	NC13-S044	631	0.1	78.60452	16.00275	−27.1‰	1230	20	1175	95	785	75
NSRL-24747	NC13-S059	640	502	78.62613	15.81750	−27.1‰	1240	20	1210	35	760	50
NSRL-24742	NC13-S048	631	30	78.60481	16.00258	−23.9‰	1295	20	1240	35	715	45
NSRL-24751	NC13-S012	436	0.2	78.64961	18.53724	−30.5‰	1295	25	1240	50	715	45
NSRL-25297	NC13-S043	630	0.1	78.60451	16.00268	−23.9‰	1295	15	1245	45	715	45
NSRL-24746	NC13-S058	623	510	78.62434	15.81826	−25.5‰	1325	20	1270	10	685	15
NSRL-25293	NC13-S033	721	8	78.11214	16.25710	−20.8‰	1330	15	1280	10	675	10
NSRL-24202	NC13-S054	589	479	78.62405	15.82580	−25.9‰	1565	20	1470	60	480	55
NSRL-24744	NC13-S055	600	482	78.62429	15.82422	−25.3‰	1580	20	1470	60	480	55
NSRL-24200	NC13-S050	684	0.5	78.60280	16.12119	−28.7‰	1605	20	1475	70	470	60
NSRL-25298	NC13-S051	687	900	78.60270	16.12342	−25.7‰	1605	15	1465	60	470	60
NSRL-24745	NC13-S057	613	491	78.62460	15.82184	−23.0‰	1735	20	1650	45	300	40
NSRL-24743	NC13-S049	682	0.5	78.60269	16.12105	−23.4‰	1745	20	1660	45	295	40
NSRL-24207	NC13-S011	462	0	78.67887	18.72580	−27.7‰	1760	20	1660	60	285	40
NSRL-24215	NC13-S032	611	5	78.10712	17.03003	−24.6‰	1770	20	1665	75	275	40
NSRL-24750	NC13-S009	569	0.5	78.70941	18.78569	−21.6‰	2370	20	2370	35		
NSRL-24203	NC13-S060	642	505	78.62727	15.81509	−25.4‰	2740	25	2825	30		
NSRL-24755	NC13-S024	683	2	77.85670	16.98846	−21.1‰	3250	20	3470	50		
NSRL-25288	NC13-S006	571	0	78.70913	18.78667	−21.3‰	3255	15	3470	45		
NSRL-24756	NC13-S026	687	0	77.87421	16.95621	−24.6‰	3260	20	3480	50		
NSRL-24212	NC13-S025	673	0.1	77.85793	16.98110	−24.5‰	3490	20	3765	55		
NSRL-24216	NC13-S034	722	4	78.11213	16.25720	−27.4‰	3585	20	3885	30		
NSRL-24758	NC13-S035	723	5	78.11214	16.25690	−22.5‰	3655	20	3970	70		
NSRL-24206	NC13-S007	568	0	78.70938	18.78562	−32.6‰	Fm: 1.0533	0.0023	Post 1950			
NSRL-24209	NC13-S017	529	0.25	78.31926	18.55959	−31.3‰	Fm: 1.0404	0.0023	Post 1950			
NSRL-24213	NC13-S027	661	3	77.95815	16.63764	−32.1‰	Fm: 1.0604	0.0024	Post 1950			
NSRL-24214	NC13-S028	662	3	77.95811	16.63757	−32.8‰	Fm: 1.0538	0.0025	Post 1950			
NSRL-24753	NC13-S017	529	0.25	78.31926	18.55959	−27.9‰	Fm: 1.0514	0.0024	Post 1950			
NSRL-24757	NC13-S030	793	0	77.94279	16.84266	−27.4‰	Fm: 1.0116	0.0022	Post 1950			
NSRL-25292	NC13-S029	792	0.5	77.94274	16.84275	−27.3‰	Fm: 1.0455	0.0018	Post 1950			

The six oldest samples (6, 24, 25, 26, 34, 35, Table 1) have ages between 4.0 and 3.4 ka, reflecting the earliest evidence of Neoglacial snowline depression in our dataset. These samples come from three different ice caps, separated by over 100 km, and were replicated at two of the ice caps. Samples 24 and 26, which have statistically indistinguishable ages, are from the same ice cap, but were collected 2.1 km apart. It is likely that the Svalbard cryosphere was expanding earlier than indicated by these dates, as the plants were collected at the margins of large, extant ice caps. As these ice caps continue to recede, they may expose even older plants in future years.

Only two samples returned ages (discordant) between the series of samples dating between 4.0 and 3.4 ka and the next series of ages beginning about 1.7 ka. The paucity of dates during the intervening interval suggests that there was little or no sustained snowline depression between 3.4 ka and 1.7 ka. This conclusion is likely robust despite the relatively small size of our dataset; with six collections between 3.4 ka and 4.0 ka and 15 collections between 1.7 and 1.0 ka, the likelihood of grossly under-sampling the intervening interval by chance is small.

Three distinct age series occur in the first millennium AD. During these intervals snowline lowered and ice margins expanded entombing living plants. The oldest of the series, between 240 and 340 AD includes 4 dates, each from a different ice cap (samples 11, 32, 49, 57). A slightly younger series of four dates (samples 50, 51, 54, 55) between 410 and 540 AD is indicative of additional snowline lowering, although the samples come from only two ice caps just 7 km apart. The final grouping in the first millennium AD consists of seven dates that cluster between 670 and 770 AD. The dates are from unique collections (12, 33, 42, 44, 48, 58, 59) at four different ice caps, including three dates at, and slightly beyond a glacier margin that document an ice advance at that time (see

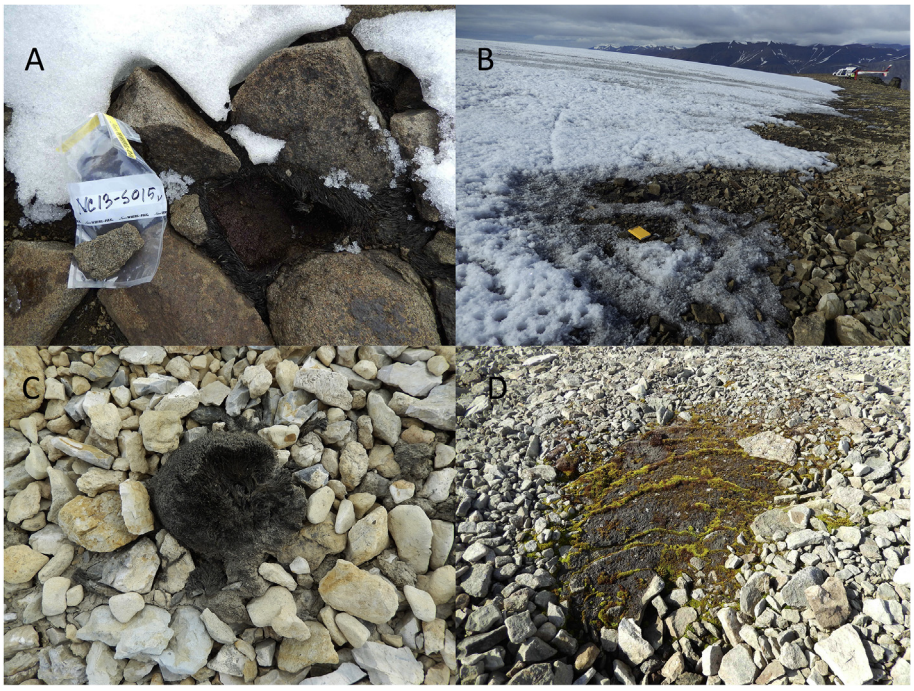

Fig. 4. Examples of recently exposed tundra vegetation. A) Ice-edge collection (NC13-S015v); B) Glacier margin with dead moss next to field book (NC13-S026); C) Moss protected from meltwater erosion 60 m from current ice margin (NC13-S047); D) Moss regrowth 5 m from the ice margin (not sampled).

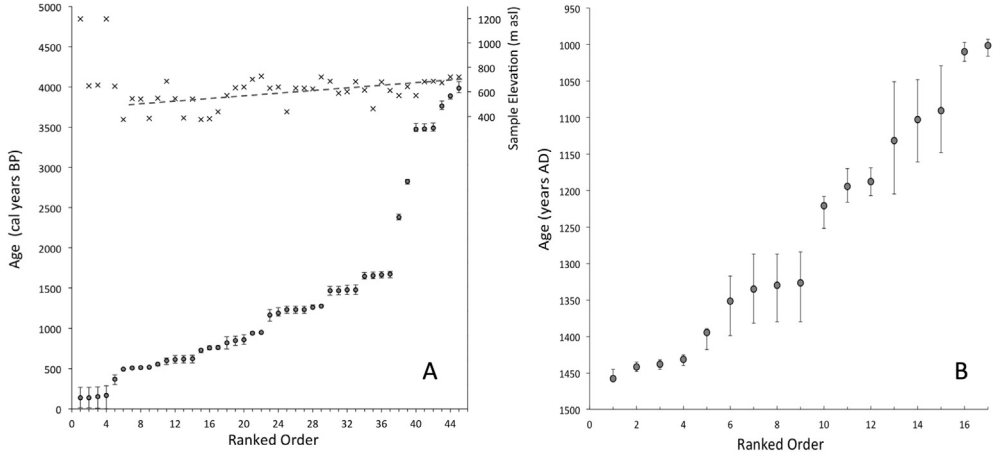

Fig. 5. All 45 non-modern dates in ranked order by calibrated years BP (median, ±1σ range) showing distinct breaks that define groups of moss-kill ages. A) Collection elevation (±10 m) is shown on the second y-axis. Omitting the five most recent and poorly constrained calendar ages, the dates show a statistically significant dependence on elevation of collection ($r = 0.62$, $p < 0.01$), with younger ages at lower collection elevations. The regression suggests an overall decrease in moss kill elevation of ~200 m over the past 4 ka. B): An expansion of the 450–1000 BP time interval in 5A, expressed in years AD.

Acknowledgements). The lack of any dated samples between 770 and 1000 AD suggests no persistent summer cooling occurred during this interval.

Seventeen samples that returned median ages between 1000 and 1450 AD reflect the transition into, and variations within the LIA. Eight samples with dates between 1000 and 1250 AD define a broad series of kill ages. This series contains three overlapping dates with small uncertainties average 1210 ± 40 AD. A century break separates the older eight samples from the nine younger samples, which indicate renewed snowline lowering beginning about 1330 AD. The four youngest dates in this group cluster tightly at 1440 ± 20 AD, a time of pronounced summer cooling recognized around the NH (Moberg et al., 2005). Five younger ages fall in a portion of the calibration curve with broad, multimodal calendar age solutions. They likely reflect ice margin variability within the late LIA, but the non-unique calendar age solutions prohibit a more detailed conclusion.

Overall, these results provide direct evidence of episodic snowline depression and summer cooling superimposed on an overall summer cooling trend over the past 4 ka. Our oldest cluster, 4.0 to 3.4 ka, represents an early Neoglacial expansion of glaciers in response to cooler summers. If summer temperatures subsequently returned to their previous levels for a sustained period those ice caps would have receded behind their 4 ka margins, newly exposed dead plants would have been removed by erosion, and the freshly deglaciated landscape would have been recolonized within a few decades after re-exposure, effectively erasing the record of the original snowline lowering. The lack of dates between 3.4 ka and 1.7

ka suggests that any summer cooling that occurred during that interval was followed by a return to warmer conditions and ice-margin retreat, with vegetation recolonizing the formerly glaciated landscape. Using the same logic, successively younger age clusters apparent in Fig. 5 each require subsequent summers to have been cooler than those prior to ice expansion on a multi-decadal average.

5.2. Relative snowline and equilibrium line altitude change

For mountain ice caps, snowline and equilibrium line altitude (ELA) are approximately coincident. In order to reconstruct the history of relative changes in snowline/ELA from our results, we first aggregate calendar age solutions (Bronk Ramsey et al., 2012) for all non-modern samples by summing the individual probability density functions (PDFs) for each date to obtain a normalized estimate of calendar age probability for all measurements as a single time series (Fig. 6). The composite series contains distinct peaks characterized by steep sides that punctuate intervals of near-zero probability corresponding to age breaks in Fig. 5. We use the peaks of probability to guide our estimate of the timing of relative change in regional ELA based on the assumption that the start of each peak defines the beginning of a moss kill interval arising from renewed descent of the snowline. We arbitrarily define the beginning and end of age probability peaks as the endpoints of line segments corresponding to the full peak width at average half height from the baseline (roughly equivalent to ±1.2 standard deviations for a normal distribution). For purposes of further highlighting the timing of relative ELA changes, we also specify brief recoveries at the end of each moss kill interval; although our results do not necessarily require a sudden rise in the ELA at the end of each interval they do indicate a cessation of anomalous snowline descent by those times. Our approach most reliably identifies the timing of initiation of anomalous cooling and related snowline depression, whereas the timing of cessation (and, hence, also the duration) of snow line lowering events is less certain, since the youngest kill dates in any single population may in some cases record ice still advancing after the cessation of climate forcing. However, we note that, based on the typical duration of events (from ±1.2 s.d. ranges above and in Fig. 6), delays of ice response cannot have been more than a few decades.

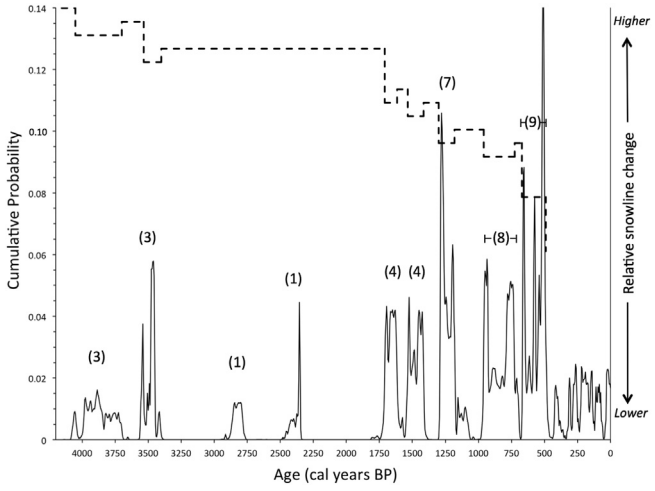

Fig. 6. Summed and normalized calendar age probability for all 45 non-modern radiocarbon dates in this study as a single composite series in calendar years before present. Number of dated samples for each broad peak, as defined in the text, is shown in parentheses. The relatively low probability peaks younger than 500 BP are largely the result of broad, multi-modal calendar age solutions for the interval and are not considered informative. Dashed line represents the relative change in snowline/ELA over the past 4 ka, as explained in the text. Some kill dates are coincident with snowline depression, whereas others may reflect expansion of ice across the kill site soon after.

Several studies have cautioned that peaks of calendar age probability and their composites may arise as a result of the non-linear structure of the ^{14}C-age:calendar-age relationship that defines the ^{14}C calibration curve (c.f. Armit et al., 2013), but also the detailed counter arguments of Margreth et al. (2014 and Supplementary Information therein). For our Svalbard data set, detailed comparisons of each of two 2-ka-long composite probability series with a synthetic data set corresponding to the aggregate normalized PDF for a ^{14}C age series with uniform 10-year spacing shows that most broad peaks produced by our collections are not controlled by the calibration process (Fig. 7). The heights of individual peaks in the interval 1000 AD to 1440 AD coincide at times with inherently increased probabilities from the calibration process, but are separated into two broad groups by an interval of zero probability ~1250 AD, an interval when the probabilities arising from calibration are elevated (Fig. 7B). In the composite series for the oldest 2 ka (Fig. 7A), only the narrow maximum at ~2.4 ka reflects a strong influence from the calibration process. Overall, the calibration process amplifies the heights of narrow peaks within the series but rarely controls the timing of baseline departures or the full width of peaks at average half height.

5.3. Time-distance diagram from a 250 m transect of well-preserved dead plants

Previous studies indicated that in most settings where entombed moss is exposed by receding ice margins, the dead plants are efficiently removed from the landscape within a few years of exposure by running water near the ice edge in summer and wind-blown snow in winter (Miller et al., 2013a). In locations where running water is at a minimum and recolonization is inhibited due to the absence of soil, with its nutrients, water holding capacity, and substrate for plant roots, we have encountered rare dead moss preserved hundreds of meters beyond current ice margins. As we will show below, such moss collections deliver successive radiocarbon ages indicating that they were killed by progressive ice advance and not by random chance unrelated to snowline change.

A series of six dead moss (samples 43–48) were collected along a 250 m upslope transect away from the 2013 AD ice edge of a small (~4 km^2) ice cap on central Spitsbergen that feeds several outlet glaciers (Fig. 8A). Collectively, they allow construction of a time-distance diagram that documents episodic ice expansion during the past 1300 years (Fig. 9). Two moss samples collected <10 m apart at the ice edge (samples 43, 44; 630 m asl) returned statistically indistinguishable calibrated ages (790 ± 40 AD and 720 ± 45 AD). At sites 45 to 48 we located infrequent, formerly ice-entombed moss that remained partially intact (Fig. 8B) up to 250 m from the 2013 AD ice edge. The derived time-distance diagram (Fig. 9) shows that ~750 AD the glacier was advancing across its 2013 AD margin and continued to advance at least another 30 m across site 48 (720 ± 45 AD; 631 m asl), where the date is indistinguishable from the two ice-edge dates. But the ice did not advance as far as site 47, another 30 m from the ice margin, or if it did, it subsequently retreated behind site 47, where the moss age is 1090 ± 60 AD. A second episode of ice expansion occurred ~1100 AD, when the ice advanced at least 60 m, rapidly crossing both sites 47 (1090 ± 60 AD; 633 m asl) and 46 (1100 ± 55 AD: 639 m asl). The final advance recorded by the dates on this transect began before 1550 AD, when moss from the most distant site (sample 45: 1580 ± 60 AD; 646 m asl), 250 m from the 2013 AD ice edge, was entombed by ice. Recession from a yet-to-be-defined LIA maximum began in the late

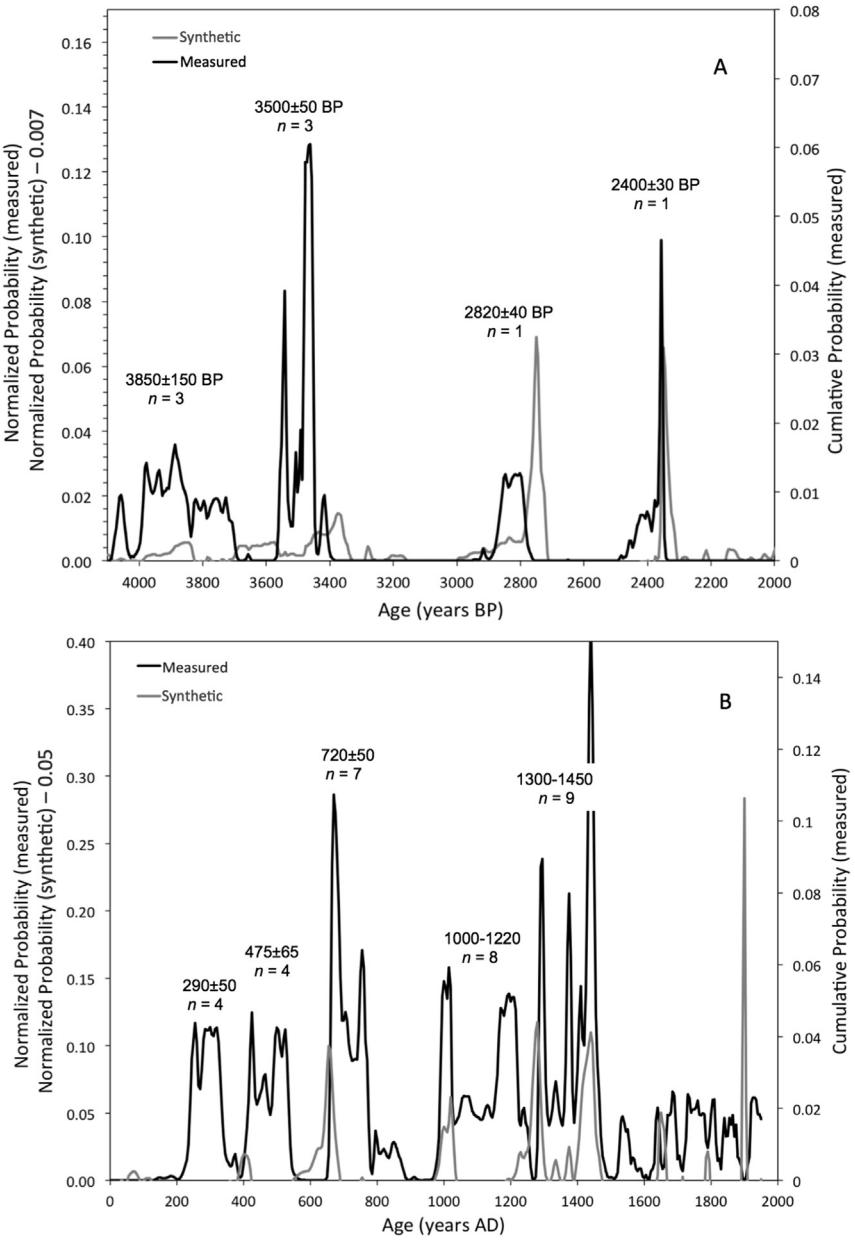

Fig. 7. Summed and normalized calendar age probability for Svalbard results (dark lines) compared with that for a synthetic, uniform series of ^{14}C ages (light lines) for the period 4.5–2.0 ka BP (A) and 0–2000 AD (B), all on the calibrated timescale. Svalbard results are as in Fig. 6. Simulated results are for a synthetic ^{14}C age series (one age ± 20 ^{14}C years every ten years) to represent the potential influence of the calibration process on the measurement results. The simulated data series is offset to emphasize the changes in probability arising from the calibration process alone. All normalized values are ×100 for ease of scaling.

19th or early 20th Century, possibly as late as 1920 AD (Nuth et al., 2013); Fig. 2). Between late August 2010 and late July 2013 photogrammetry shows that the ice margin retreated ~20 m, a retreat rate of ~5 m a^{-1}. Extrapolating over the full 250 m of plant preservation suggests the farthest site from the ice edge (sample 45) emerged from beneath the ice at least 50 years ago. Collectively, these observations suggest the dead moss along this transect was exposed but remained intact for at least 50, but probably not more than 90 years. We cannot tell whether discontinuities in the moss dates represent ice-margin stasis, or ice recession due to relatively warmer summers. Although our data carry no information on the extent of ice recession between advances, they do require that stepped ice-expansion dominated that interval. These episodes of ice advance (~750, ~1100 and before 1550 AD) appear to correspond with moss kill intervals indicated by the composite probability series for all samples (670–770, 1000 to 1220, and ~1450 to ~1900 AD; Fig. 7B[1]), supporting our argument that distributed moss kill ages reflect regional snowline depression and ice advance. The time-distance diagram also demonstrates that the progressive ice margin advance over ~1200 years was erased in less than a century as summers warmed after 1920 AD (Fig. 2), and that glaciers attained their greatest Neoglacial dimensions during the LIA. The retreat since ~1920 AD suggests that the last century was the warmest since the 8th century AD, including medieval times.

It is possible that relict plants found some distance beyond current ice margins, such as those described above, might be re-

[1] Fig. 7 includes the transect dates, but the Correspondence is equally strong with all transect dates removed (Fig. S1).

entombed by subsequent ice expansion. This may explain why at five of our sites adjacent moss clumps at the ice edge returned discordant radiocarbon ages, unlike typically concordant ages reported for nearby ice-edge plants collected in Arctic Canada (LaFarge et al., 2013; Miller et al., 2013b; but see also Margreth et al., 2014). Another possible explanation for the range of ages at some sites is that this reflects the slow growth of mosses (Humlum et al., 2005). However, as mosses grow from one end, they die at the other, and decomposition of the dead portions, while slower in the Arctic than at lower latitudes, is not likely to explain the large age ranges observed at some ice-margin sites. We tested the potential impact of slow growth/decay in Baffin Island samples, a region with colder summers than on Svalbard. A single full stem of living *Polytrichum* moss was radiocarbon dated and found to be in equilibrium with atmospheric $^{14}CO_2$ levels of the preceding 5 years, and in another test, we dated three different stems from a single *Polytrichum* clump killed over 1000 years ago, with all three ages agreeing within the small analytical uncertainties (Miller et al., 2013a). Consequently, we interpret all our ages to represent kill dates related to an expanding cryosphere, even when multiple ages are present in nearby collections.

6. Discussion

6.1. Other Svalbard records

Humlum et al. (2005) report eleven ^{14}C dates on *in situ* dead moss recovered beneath Longyearbreen, central Spitsbergen (Fig. 3). Comparing a composite PDF of those dates with the PDF from this study (Fig. 10) shows similarities; in particular, peaks at 675 and 760 AD appear in both PDFs and are not present in the inherent structure of the calibration curve (Fig. 7B). The lack of clustered ages earlier in the first millennium AD in the Longyearbreen data may reflect their relatively large measurement uncertainties, although there is a broad peak around 500 AD corresponding to a peak in our data set of about the same age. Accelerator precision has improved in recent years, and smaller uncertainties allow for clearer separation of peaks of calendar age probability. Because measurement uncertainties in the earlier study are about twice those for our results makes a more detailed comparison difficult. Nevertheless, the Longyearbreen samples document ice advance early in the first millennium AD, and by the peak of the LIA the glacier was almost twice the size it was prior to the first millennium AD advance, strongly supporting our interpretation that our data describe intermittent, but overall continued snowline lowering over the past 2 ka.

Other examples of entombed plant macrofossils include Lubinski et al. (1999), who report ten dates on *in situ* dead moss at and beyond ice margins on Franz Josef Land, Arctic Russia. The composite PDF of those dates incorporates their relatively large uncertainties but suggests ice expanded after 1000 AD (Fig. 10). Baranowski and Karlén (1976) report a thick tundra bed between Neoglacial tills in front of Werenskioldbreen, SW Spitsbergen (Fig. 3), from which three radiocarbon dates range from 450 ± 240 AD to 1220 ± 170 AD, indicating at least one advance/retreat cycle in the first millennium AD. Werner (1993) used lichenometry to date Neoglacial moraine stabilization, with estimated stabilization ages of ~500 AD and ~1000 AD, followed by a 2-part LIA. None of these studies has sufficient precision to compare directly with our current results, but all are consistent with our evidence that widespread Neoglacial advance and retreat cycles occurred during the past two millennia.

Sediment from Linnévatnet, a lake on the west coast of Spitsbergen (Fig. 3), records the activity of glaciers in both the main valley (Linnédalen) and in a small cirque that drains into an isolated

Fig. 8. Transect of dead moss dates used for time-distance diagram in Fig. 9. A) Locations of *in situ* dead moss extending 250 m from the 2013 AD ice edge. Median calibrated ages are given to the left of each collection site; Field IDs (Table 1) are to the right. Image: Digital Globe 25 Aug 2010; ~20 m of lateral ice recession occurred between 2010 and 2013. B) Desiccated moss clump at site 46 (1105 ± 55 AD) showing the porous rocky substrate and lack of soil that inhibited plant recolonization and restricted surface water erosion after deglaciation.

basin of the lake. Sediment cores from the central basin indicate the main valley was free of glacial erosion during the early Holocene, with small valley glaciers initially forming between 5 and 4 ka, and peak Neoglaciation after ~1200 AD (Snyder et al., 2000a; Svendsen and Mangerud, 1997). Studies of sedimentary ancient DNA from the nearby lake Skartjørna also show a transition to sparser vegetation and lower biomass between 5500 and 4000 ka (Alsos et al., 2015).

Paleo-ELA fluctuations for Karlbreen, a glacier on west Spitsbergen (Fig. 3), derived from a high-resolution physical-proxy-based lacustrine record, suggest that the glacier first formed in response to snowline depression between 4.0 and 3.5 ka, followed by substantial additional ELA depression early in the first millennium AD, with a final drop to the lowest ELA since at least 7 ka about 1450 AD (Røthe et al., 2015). Although the magnitude of the snowline depression cannot be derived directly from the vegetation kill dates, each successive cluster of kill dates reflect a snowline drop greater than the preceding cluster, consistent with the first-order trend of steadily decreasing ELA for Karlbreen, and the abundance of kill dates early in the first millennium AD is consistent with the strong decline in ELA for Karlbreen.

An 1800-year record of summer temperature derived from the alkenone unsaturation index in sediment from Kongressvatnet, a small lake above Linnévatnet (Fig. 1) shows only slight summer (JJA) cooling between ~200 AD and 1400 AD, then generally increasing temperatures after 1400 AD until ~1950 AD, followed by more rapid warming since 1950 AD (D'Andrea et al., 2015).

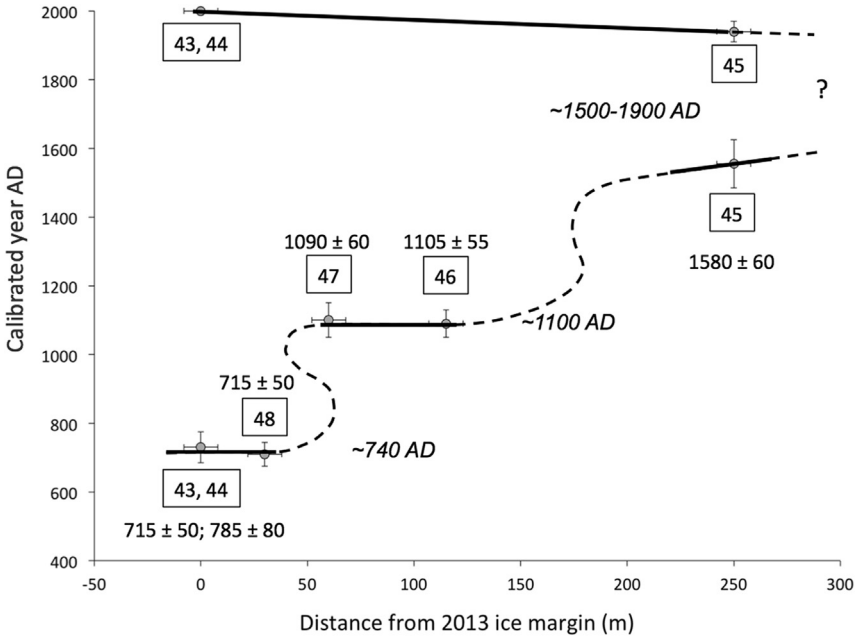

Fig. 9. Time-distance diagram derived from the positions and dates along the transect shown in Fig. 8A, illustrating the episodic expansion of the ice margin (dashed where unconstrained). Numbers in squares are Field IDs, with calibrated ages (Table 1). Locations are as recorded by conventional GPS. Uncertainties (±1σ) are given for both calibrated ages and distances.

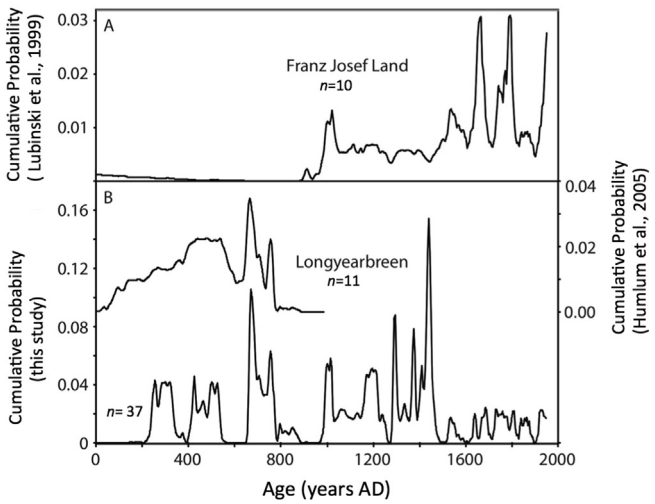

Fig. 10. Comparison of cumulative PDFs of calibrated ^{14}C ages on entombed moss. A) dead moss collected at and beyond ice margins on Franz Josef Land (Lubinski et al., 1999); (B; lower) pdf of calibrated ^{14}C ages from this work (lower) and of moss collected beneath Longyearbreen (Humlum et al., 2005). Peaks younger than 1600 AD reflect non-unique calibration solutions, hence contain little actual age information.

Reconstructed summer temperatures are 1.0–2.5 °C higher in the 1800s than during previous centuries, yet Svalbard glaciers reached their maximum Neoglacial dimensions in the 1800s. Discrepancies between the alkenone record and other records may reflect a role for increased precipitation, or may be the lack of secure calibration below 3.3 °C for the alkenone paleothermometer.

6.2. Regional comparisons

The history of Neoglaciation in coastal Norway appears to be broadly similar to the Svalbard records. A multiproxy reconstruction of ELA variation for Lenangsbreene, a glacier in north Norway (Fig. 1), identifies the Neoglacial onset of glacial erosion ~4 ka, and a step change toward even colder summers and cryosphere expansion early in the first millennium AD (Bakke et al., 2005a). Holocene variations in the ELA of Folgefonna, a glacier in western Norway (Fig. 1), reveal an early phase of Neoglacial expansion 5.2 ka, but the onset of a trend toward lower elevations began 4.5 ka, with the largest ELA decline early in the first millennium AD (Bakke et al., 2005b).

The ELA reconstructions for Karlbreen, Lenangsbreene, and Folgefonna over the past 4 ka are compared to the inferred relative ELA change based on the PDF of our emergent moss dates in Fig. 11, with all four records recording cooling between 4.0 and 3.5 ka. The ELA reconstructions indicate a slow descent from 3.5 to 2.0 ka, followed by a sharp lowering of the ELA early in the first millennium AD, then irregular continued descent through to the peak summer cold of the LIA by ~1450 AD or later, similar to our composite PDF of snowline/ELA lowering (Fig. 11A).

The climate of both western Norway and Svalbard are influenced by the presence of the warm North Atlantic Current, and it poleward extension, and West Spitsbergen Current (Aagaard and Carmack, 1994). Marine sediment cores from around Svalbard provide proxy evidence of the changing influence of the WSC through the Holocene showing that Atlantic water inflow along West Spitsbergen was relatively strong from 10.8 to 6.8 ka, diminishing to a low level by ~4 ka (Rasmussen et al., 2012; Slubowska-Woldengen et al., 2007), close to the age of our oldest moss kill dates. After ~1000 AD a range of proxies in marine sediment indicate greater upper ocean variability, generally lower upper ocean temperatures, and increased ice rafting along West Spitsbergen compared to previous millennia (Slubowska-Woldengen et al., 2007). The implied stepwise deterioration of the marine environment may have been linked in part to changes in sea-ice production in the Arctic Ocean, as the deglacial sea-level rise flooded the broad, shallow Arctic Ocean shelves (Werner et al., 2013). Changes in the poleward advection of relatively warm surface water into the Nordic Seas through the Holocene may have paced regional snowline and ELA lowering events, although a

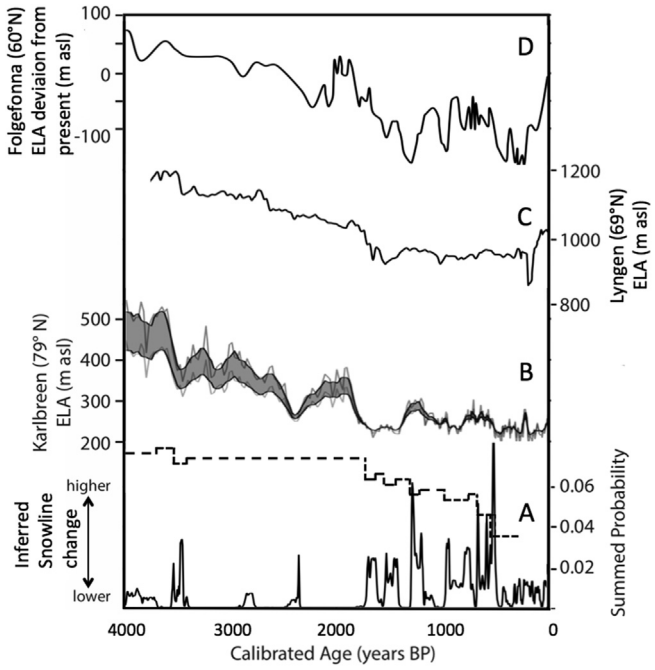

Fig. 11. Regional comparisons of paleo snowline/ELA variations over the past 4 ka. A) Snowline change inferred from composite calendar age probabilities of moss kill dates from Svalbard (this study, as in Fig. 6); B) ELA change for Karlbreen, Svalbard (Røthe et al., 2015); C) ELA change for Lenanangsbreen, north Norway (Bakke et al., 2005a); D) ELA deviations from present for Folgefonna, west Norway (Bakke et al., 2005b). All four reconstructions show snowline/ELA descent between 4.0 and 3.5 ka, with additional stepped cooling early in the first millennium AD, and during the LIA.

more direct response of regional snowline to altered radiative forcing cannot be ruled out and requires a more comprehensive analysis.

7. Conclusions

Although most glaciers on Svalbard are polythermal (Björnsson et al., 1996) and likely sliding on their beds, portions of many Svalbard glaciers are cold-based and more likely to preserve than erode the landscape. We found *in situ* tundra plants emerging beneath many Svalbard glacier margins, confirming the widespread occurrence of cold-based ice. A similar argument for widespread cold-based ice on Svalbard during the Late Weichselian glaciation has been proposed to reconcile the preservation of delicate raised beaches well inside Late Weichselian ice margins (Landvik et al., 2005; Landvik et al., 2014).

The calibrated radiocarbon ages of ice-entombed plants define past episodes of snowline/ELA lowering that led to ice expansion. Our series of 45 non-modern radiocarbon-dated plants that were entombed beneath cold-based ice indicate persistent snowline lowering began at least 4.0 to 3.4 ka. Snowlines have become progressively, but episodically, lower since then, as summer temperatures decreased, although the summers of the past century have been, on average, warmer than any century in at least the past 1.3 ka. A widespread expansion of the cryosphere on Svalbard began early in the first millennium AD, with distinct intervals of snowline lowering between 240 and 340 AD, 410 and 540 AD, and 670 and 770 AD. After a 250-year interval lacking evidence of ice expansion, renewed descent of the regional snowline occurred between 1000 AD and 1250 AD, followed by the LIA, with additional snow and ice expansion between 1300 and 1450 AD. Our signal is rectified after 1450 AD because nearly all glaciers are smaller now than at any time after 1450 AD, and non-unique calibration solutions render ambiguous kill dates younger than 1600 AD.

The regular Holocene decline of NH summer insolation was very likely the primary driver for widespread expansion of the NH cryosphere through the Holocene (Wanner et al., 2008), with maximum dimension since 8 ka achieved during the LIA. However, episodic ice expansion as evidenced by the age distribution of entombed plants on Svalbard cannot be explained by the near-linear insolation forcing alone, and would seem to require substantial internal climate variability and/or a significant response to other forcings. Episodic ice expansion ~4 ka occurred shortly after the WSC cooled and Arctic Ocean sea-ice export increased, both of which likely played a role in the initiation of an expanded cryosphere on Svalbard, and subsequent variations in its dimensions. The similarities in the onset of Neoglacial ELA depression between coastal Norway and Svalbard are consistent with episodic weakening of the North Atlantic Current through the late Holocene.

A lateral transect of vegetation kill ages confirm episodic ice cap expansion after ~700 AD to a maximum sometime between ~1500–1900 AD, followed by rapid retreat during this century. These results indicate that the last century was the warmest since at least ~700 AD, including the warmth of Medieval times. Summertime warming and ice retreat are ongoing despite a recent decrease in warm Atlantic inflow to the region, suggesting a strong regional response to increased anthropogenic climate forcing.

Acknowledgements

Our research on Svalbard builds on experience gained over more than 30 years of intermittent field studies there by all three authors. The Research Council of Norway (Svalbard Science Forum) grant ES502676 to Landvik and Miller supported the project. Our field effort benefited from experience gained searching for emerging plants in Arctic Canada and Greenland under sponsorship of the US National Science Foundation grant ARC-1204096. We thank the Norwegian Polar Institute for access to helicopter resources, and the Governor of Svalbard (Sysselmannen på Svalbard) for permission to land outside protected areas. Paul Morin and the Polar Geospatial Center (http://www.pgc.umn.edu) provided high-resolution satellite imagery that greatly aided selection of optimal collection sites. GHM thanks S. Pendleton, C Florian, and S. DeVogel for assistance in the lab and with figures. SJL thanks C. Wolak and P. Cappa for assistance with radiocarbon preparations. The manuscript benefited from thoughtful comments by S. Pendleton and S. Crump.

Appendix A. Supplementary data

Supplementary data related to this article can be found at http://dx.doi.org/10.1016/j.quascirev.2016.10.023.

References

Aagaard, K., Carmack, E.C., 1994. The Arctic Ocean and climate: a perspective. In: Johannessen, O.M., J.E.O., R.D.M.a. (Eds.), The Polar Oceans and Their Role in Shaping the Global Environment. American Geophysical Union, Washington, D. C., pp. 5–20

Alsos, I.G., Sjögren, P., Edwards, M.E., Landvik, J.Y., Gielly, L., Forwick, M., Coissac, E., Brown, A.G., Jakobsen, L.V., Føreid, M.K., 2015. Sedimentary ancient DNA from Lake Skartjørna, Svalbard: assessing the resilience of arctic flora to Holocene climate change. Holocene, 0959683615612563.

Armit, I., Swindles, G.T., Becker, K., 2013. From dates to demography in later prehistoric Ireland? Experimental approaches to the meta-analysis of large 14C data-sets. J. Archaeol. Sci. 40, 433–438.

Bakke, J., Dahl, S.O., Paasche, Ø., Løvlie, R., Nesje, A., 2005a. Glacier fluctuations, equilibrium-line altitudes and palaeoclimate in Lyngen, northern Norway, during the Lateglacial and Holocene. Holocene 15, 518–540.

Bakke, J., Lie, Ø., Nesje, A., Dahl, S.O., Paasche, Ø., 2005b. Utilizing physical sediment variability in glacier-fed lakes for continuous glacier reconstructions during the Holocene, northern Folgefonna, western Norway. Holocene 15, 161–176.
Bergsma, B.M., Svoboda, J., Freedman, B., 1984. Entombed plant communities released by a retreating glacier at central Ellesmere Island, Canada. Arctic 37, 49–52.
Björnsson, H., Gjessing, Y., Hamran, S.E., Hagen, J.O., 1996. The thermal regime of sub-polar glaciers mapped by multi-frequency radio-echo sounding. J. Glaciol. 42, 23–32.
Bronk Ramsey, C., Staff, R.A., Bryant, C.L., Brock, F., Kitagawa, H., van der Plicht, J., Schlolaut, G., Marshall, M.H., Brauer, A., Lamb, H.F., Payne, R.L., Tarasov, P.E., Haraguchi, T., Gotanda, K., Yonenobu, H., Yokoyama, Y., Tada, R., Nakagawa, T., 2012. A complete terrestrial radiocarbon record for 11.2 to 52.8 kyr B.P. Science 338, 370–374.
Chylek, P., Folland, C.K., Lesins, G., Dubey, M.K., Wang, M., 2009. Arctic air temperature change amplification and the Atlantic Multidecadal Oscillation. Geophys. Res. Lett. 36, L1480.
D'Andrea, W.J., Vaillencourt, D.A., Balascio, N.L., Werner, A., Roof, S.R., Retelle, M., Bradley, R.S., 2012. Mild Little Ice Age and unprecedented recent warmth in an 1800 year lake sediment record from Svalbard. Geology 40, 1007–1010.
Falconer, G., 1966. Preservation of vegetation and patterned ground under a thin ice body in northern Baffin Island, N.W.T. Geogr. Bull. 8, 194–200.
Hagen, J.O., Kohler, J., Melvold, K., Winther, J.-G., 2003. Glaciers in Svalbard: mass balance, runoff and freshwater flux. Polar Res. 22, 145–159.
Hagen, J.O., Liestøl, O., Roland, E., Jørgensen, T., 1993. Glacier Atlas of Svalbard and Jan Mayen, p. 169. Meddelelser. Norsk Polarinstitutt.
Hobbs, R.J., Mallik, A.U., Gimingham, C.H., 1984. Studies on fire in Scottish heathland communities. III. Vital attributes of the species. J. Ecol. 72, 963–976.
Humlum, O., Elberling, B., Hormes, A., Fjordheim, K., Hansen, O.H., Heinemeier, J., 2005. Late-Holocene glacier growth in Svalbard, documented by subglacial relict vegetation and living soil microbes. Holocene 15, 396–407.
Humlum, O., Solheim, J.E., Stordahl, K., 2011. Spectral analysis of the Svalbard temperature record 1912–2010. Adv. Meteorol.
Hurrell, J.W., Deser, C., 2010. North Atlantic climate variability: the role of the North Atlantic oscillation. J. Mar. Syst. 79, 231–244.
James, T.D., Murray, T., Barrand, N.E., Sykes, H.J., Fox, A.J., King, M.A., 2012. Observations of enhanced thinning in the upper reaches of Svalbard glaciers. Cryosphere 6, 1369–1381.
LaFarge, C., Williams, K.H., England, J.H., 2013. Regeneration of Little Ice Age bryophytes emerging from a polar glacier with implications of totipotency in extreme environments. PNAS 110, 9839–9844.
Landvik, J.Y., Alexanderson, H., Henriksen, M., Ingolfsson, O., 2014. Landscape imprints of changing glacial regimes during ice-sheet build-up and decay: a conceptual model from Svalbard. Quat. Sci. Rev. 92, 258–268.
Landvik, J.Y., Bondevik, S., Elverhøi, A., Fjeldskaar, W., Mangerud, J., Salvigsen, O., Siegert, M.J., Svendsen, J.-I., Vorren, T.O., 1998. The last glacial maximum of Svalbard and the Barents Sea area: ice sheet extent and configuration. Quat. Sci. Rev. 17, 43–75.
Landvik, J.Y., Ingólfsson, Ó., Mienert, J., Lehman, S.J., Solheim, A., Elverhøi, A., Ottesen, D., 2005. Rethinking late Weichselian ice-sheet dynamics in coastal NW Svalbard. Boreas 34, 7–24.
Lowell, T.V., Hall, B.L., Kelly, M.A., Bennike, O., Lusas, A.R., Honsaker, W., Smith, C.A., Levy, L.B., Travis, S., Denton, G.H., 2013. Late Holocene expansion of istorvet ice cap, Liverpool land, east Greenland. Quat. Sci. Rev. 63, 128–140.
Lubinski, D.J., Forman, S.L., Miller, G.H., 1999. Holocene glacier and climate fluctuations on Franz Josef land, arctic Russia, 80°N. Quat. Sci. Rev. 18, 85–108.
Margreth, A., Dyke, A.S., Gosse, J.C., Telka, A.M., 2014. Neoglacial ice expansion and late Holocene cold-based ice cap dynamics on Cumberland Peninsula, Baffin Island, Arctic Canada. Quat. Sci. Rev. 91, 242–256.
McCartney, M.S., Curry, R.G., Bezdek, H.F., 1996. North Atlantic's transformation pipeline chills and redistributes subtropical water. Oceanus 39, 19–23.
Miller, G.H., Briner, J.P., Refsnider, K.A., Lehman, S.J., Geirsdottir, A., Larsen, D.J., Southon, J.R., 2013a. Substantial agreement on the timing and magnitude of Late Holocene ice cap expansion between East Greenland and the Eastern Canadian Arctic: a commentary on Lowell et al. Quat. Sci. Rev. 77, 239–245.
Miller, G.H., Lehman, S.J., Refsnider, K.A., Southon, J.R., Zhong, Y., 2013b. Unprecedented recent summer warmth in Arctic Canada. Geophys. Res. Lett. 40, 1–7.
Moberg, A., Sonechkin, D.M., Holmgren, K., Datsenko, N.M., Karlén, W., 2005. Highly variable Northern Hemisphere temperatures reconstructed from low- and high-resolution proxy data. Nature 433, 13–17.
Nordli, Ø., Przybylak, R., Ogilvie, A.E.J., Isaksen, K., 2014. Long-term Temperature Trends and Variability on Spitsbergen: the Extended Svalbard Airport Temperature Series, 1898-2012. 2014.
Nuth, C., Kohler, J., König, M., Deschwanden, A.v., Hagen, J., Kääb, A., Moholdt, G., Pettersson, R., 2013. Decadal changes from a multi-temporal glacier inventory of Svalbard. Cryosphere 7, 1603–1621.
Rahmstorf, S., Feulner, G., Mann, M.E., Robinson, A., Rutherford, S., Schaffernicht, E.J., 2015. Exceptional twentieth-century slowdown in Atlantic Ocean overturning circulation. Nat. Clim. change 5, 475–480.
Rasmussen, T.L., Forwick, M., Mackensen, A., 2012. Reconstruction of inflow of Atlantic water to isfjorden, Svalbard during the Holocene: correlation to climate and seasonality. Mar. Micropaleontol. 94–95, 80–90.
Reusche, M., Winsor, K., Carlson, A.E., Marcott, S.A., Rood, D.H., Novak, A., Roof, S., Retelle, M., Werner, A., Caffee, M., Clark, P.U., 2014. 10Be surface exposure ages on the late-Pleistocene and Holocene history of Linnebreen on Svalbard. Quat. Sci. Rev. 89, 5–12.
Røthe, T.O., Bakke, J., Vasskog, K., Gjerde, M., D'Andrea, W.J., Bradley, R.S., 2015. Arctic Holocene glacier fluctuations reconstructed from lake sediments at Mitrahalvøya, Spitsbergen. Quat. Sci. Rev. 109, 111–125.
Slubowska-Woldengen, M., Rasmussen, T.L., Koc, N., Klitgaard-Kristensen, D., Nilsen, F., Solheim, A., 2007. Advection of Atlantic Water to the western and northern Svalbard shelf since 17,500 cal yr BP. Quat. Sci. Rev. 26, 463–478.
Snyder, J.A., Werner, A., Miller, G.H., 2000a. Holocene cirque glacier activity in western Spitsbergen, Svalbard: sediment records from proglacial Linne vatnet. Holocene 555–563.
Snyder, J.A., Werner, A., Miller, G.H., 2000b. Holocene cirque glacier activity in western Spitsbergen, Svalbard: sediment records from proglacial Linne vatnet. Holocene 10, 555–563.
Svendsen, J.I., Mangerud, J., 1997. Holocene glacial and climatic variations on Spitsbergen, Svalbard. Holocene 7, 45–57.
Wanner, H., Beer, J., Bütikofer, J., Crowley, T.J., Cubasch, U., Flückiger, J., Goosse, H.M., Joos, F., Kaplan, J.O., Küttel, M., Müller, S.A., Solomina, O., Stocker, T.F., Tarasov, P.E., Wagner, M., Widmann, M., 2008. Mid- to Late Holocene climate change: an overview. Quat. Sci. Rev. 27, 1791–1828.
Werner, K., Spielhagen, R.F., Bauch, D., Hass, C., Kandiano, E., 2013. Atlantic Water advection versus sea-ice advances in the eastern Fram Strait during the last 9 ka: multiproxy evidence for a two- phase Holocene. Paleoceanography 28, 283–295.